PARAMETRIC SCALING OF TURBULENT IMPINGING JETS OVER SMOOTH SURFACES

Juliana B. R. Loureiro, jbrloureiro@gmail.com
Atila P. Silva Freire, atila@mecanica.coppe.ufrj.br
Mechanical Engineering Program (COPPE/UFRJ),
C.P. 68503, 21945-970, Rio de Janeiro, RJ, Brazil,

Abstract. *This work investigates the validity of some parametric scaling equations for the description of turbulent impinging jets over smooth surfaces. An experimental campaign was performed with the aid of a Laser-Doppler Anemometer system. Results show mean velocity and higher order distributions at different radial positions of the impingement plate. Two different parametric analyses are made. The first analysis resorts to classical variables of the problem, including the nozzle diameter, nozzle-to-plate space and bulk velocity of the jet. The second approach considers only gross parameters of the jet. The parametric predictions are evaluated against the experimental results.*

Keywords: *Turbulence, impinging jet, laser-Doppler anemometry, parametric analysis*

1. INTRODUCTION

The typical geometry of a confined turbulent impinging jet is characterized by three regions: i) the region of free jet, located immediately downstream of the issuing nozzle, ii) the stagnation region, where streamlines are highly deflected laterally and iii) the wall jet region, where the flow behaves as a boundary layer that develops along the impingement plate. Given their peculiar features, impinging jets can be used in a myriad of industrial applications that require some form of heating or cooling. Examples are the tempering of glass and metal sheets, the drying process of paper and textiles and the cooling of electronic components.

From a fundamental perspective, impinging jets are also an interesting problem. The presence of a stagnation point, the sharp curvature of streamlines and high velocity gradients near the surface are aspects that pose some serious difficulties for the numerical modeling of the problem as well as for any experimental techniques intended at quantifying the jet properties. Despite the many works devoted to turbulent jets that can be found in the literature, some important issues still require a proper assessment. The present work tackles two of those important problems: i) the need for accurate wall shear measurements for theoretical and numerical validation purposes and ii) the development of a parametric analysis for the mean flow field and second order moments.

The near wall measurements for a smooth impingement surface were performed through laser Doppler anemometry. Results were used to evaluate the wall shear stress – τ_w – by means of the linear mean velocity profile in the viscous sublayer (Loureiro et al., 2010). A scaling analysis of the mean and turbulent velocities was made based on procedures that took into account conventional parameters such as the nozzle diameter, the nozzle-to-plate distance and the bulk velocity of the jet. Alternatively, a second scaling analysis procedure was performed considering some gross parameters of the flow. The near wall logarithmic solution written in terms of the parameters proposed by Özdemir and Whitelaw (1992) was also investigated.

2. SCALING ANALYSIS

Regarding wall jets, Özdemir and Whitelaw (1992) proposed a functional behaviour for the log-law intercept, A, that uses a scaling procedure based on the stream-wise evolution of the flow characterized by its maximum velocity, U_{max}. The important contribution of this work was the recognition that the nozzle diameter is an inappropriate reference scaling.

Thus, local similarity must take into account the flow evolution with an expression of the form:

$$\frac{u}{u_\tau} = \frac{1}{\varkappa} \ln\left(\frac{y u_\tau}{\nu}\right) + A, \qquad \text{with} \qquad A = A_1 \frac{U_{max}}{u_\tau} - A_2, \tag{1}$$ eq:lw1

where $\varkappa = 0.4$, u_τ denotes the friction velocity and A_1 and A_2 are constants.

In addition, the work of Özdemir and Whitelaw (1992) has also suggested that a Weibull distribution, written in the form

$$\frac{u}{U_{max}} = \frac{\eta}{\beta}\left(\frac{y/y_{0.5}}{\beta}\right)^{\eta-1} \exp\left(-\left(\frac{y/y_{0.5}}{\beta}\right)^{\eta}\right), \tag{2}$$ eq:weibu

might represent well some of the global features of the mean velocity profile, such as the position of the maximum and of the outer inflection point ($y_{0.5}$). However, a Weibull distribution is not a suitable approximation in the near wall region, since it furnishes an infinite wall shear stress.

The representation of the inner flow thus requires the development of correlations capable of describing the behaviour of U_{max} and its position, y_{max}, as a function of the radial distance. For unconfined turbulent wall jets, many authors have proposed to correlate the results through power law expressions with the forms,

$$\frac{U_{max}}{U_o} = B_1\left(\frac{r}{D}\right)^{n_1}, \qquad \frac{y_{max}}{D} = B_2\left(\frac{r}{D}\right)^{n_2}. \tag{3}$$ eq:umax

Values quoted for parameters B_1, B_2, n_1 and n_2 vary greatly according to flow conditions.

The choice of U_{max} and D as the basic flow scales has been challenged by Narasimha et al. (1973) with the argument of selective memory. These authors reason that sufficiently downstream in turbulent flows "the details of the initial conditions are not relevant, but rather only a few gross parameters which are in some sense dynamically equivalent". The natural implication is that Eqs. (3) are re-written as

$$\frac{U_{max}\nu}{M_j} = C_1\left(\frac{rM_j}{\nu^2}\right)^{m_1}, \quad M_j = DU_o^2, \qquad \frac{y_{max}M_j}{\nu^2} = C_2\left(\frac{rM_j}{\nu^2}\right)^{m_2}. \tag{4}$$ eq:umax_

The Reynolds shear stresses in turbulent boundary layers have always been correlated in terms of wall variables – that is to say in terms of u_τ – so that similarity can be assessed. Here, to correlate u'_{rms}, two other characteristic velocities can be used: U_{max} and U_o. As the peak in u'_{rms} moves away from the wall, the outer flow reference velocities should be used. The positions at which the u'-profiles reach the outer maximum, y'_{max}, are also of interest to the present analysis and can be correlated in analogy to Eqs.(3). Eventually, an analysis based on the gross parameters proposed by Narasimha et al.(1973) can also be attempted to correlate $(u'_{rms})_{max}$ and y'_{max}.

For the wall jet region, the empirical expression of Poreh et al. (1967) for the mean shear stress in a radial wall jet,

$$\frac{\tau_w}{\rho U_o^2} = 0.34 R_D^{-3/10}\left(\frac{D}{H}\right)^2\left(\frac{r}{H}\right)^{-2.3}, \tag{5}$$ eq:twpor

will be tested against the present experimental results.

3. EXPERIMENTAL SET UP AND MEASUREMENT TECNIQUES

The present results were obtained for a jet issuing from a circular nozzle with a bulk velocity, U_o = 17 ms^{-1}, as illustrated in Fig. 1. These conditions give a Reynolds number based on jet nozzle diameter, R_D, equal to 47,100. The impingement smooth flat surface was made of a plexiglass plate with 840 mm in diameter. Only one nozzle-to-plate

spacing was considered in the experiments, H/D = 2.

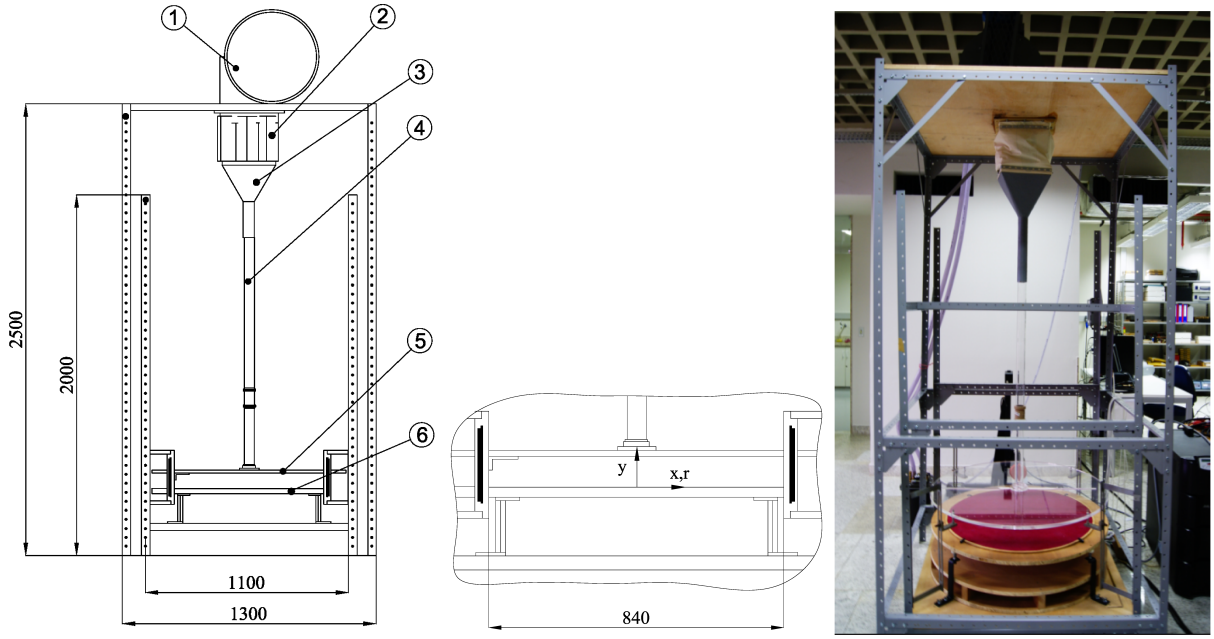

Figure 1. General arrangement of the experimental set up: (a) descriptive drawing including (1) centrifugal blower, (2) flexible transition section, (3) contraction, (4) flow pipe, (5) confinement plate, (6) impingement plate; (b) schematic detail showing the coordinate system; (c) photograph. Dimensions are shown in mm.

fig:exps

The Dantec Dynamics two-channel laser-Doppler anemometer used a 400 mW Ar-ion tube laser and was operated in the forward-scatter mode for one velocity component measurement. A series of LDA biases were avoided by the use of transit time weighting and by adjusting the strictest parameters on the data processor and software.

As an additional method for wall shear stress measurements, the present work used surface Pitot tubes with external diameters of 0.38, 1.26, 1.65 and 3.18 mm. For data reduction, the calibration curves of Patel were used. Pressure measurements were obtained through a Furness micromanometer, that provided an accuracy of 0.001 Pa.

4. RESULTS AND DISCUSSION

Mean velocity profiles along the impingement plate are shown in Fig. 2a normalized by the local maximum velocity and its distance from the wall ($y_{0.5}$). The similarity fit obtained with the Weibull distribution is also shown. Although the mean velocity profile seems to be well represented by the Weibull distribution, the shear stress calculated from this distribution blows out as y approaches the wall. For this region, the logarithmic relation shown in Eq. (1) must be used (Fig. 2b).

The linear behaviour of the additive constante of the logarithmic law A (Eq. (1)) observed from the experimental results is used to determine A_1 (= 0.962) and A_2 (= -8.987). These values are compared with the results of Özdemir and Whitelaw (1992) and Guerra et al. (2005) in Table 1. As a whole, the values in Table 1 are very consistent: A_1 has a value most probably near unity and A_2 around 9. The large variation in values that, for example, Narasimha et al. (1973) describe for the coefficients and exponents in correlations such as Eqs. (3) is not observed for the values shown in Table 1. The relevant conclusion is that the functional behaviour of the additive parameter in the law of the wall for impinging jets over smooth surfaces seems to follow Eq. (6),

$$A = 0.962\frac{U_{max}}{u_\tau} - 8.987. \qquad (6)$$

eq:c

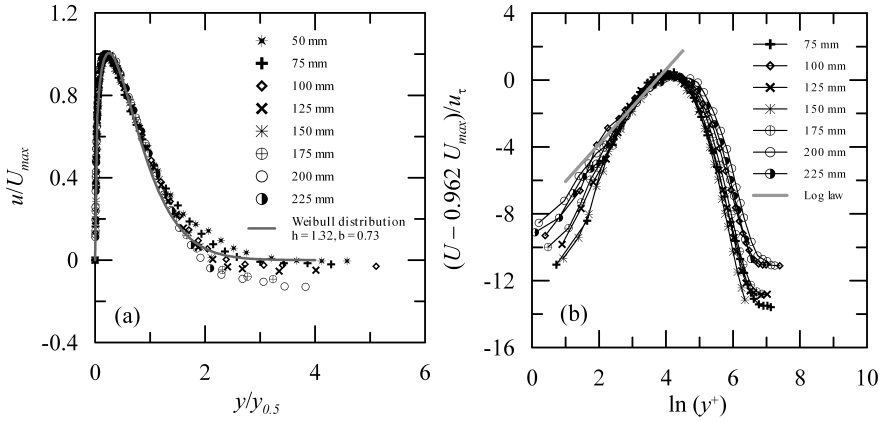

Figure 2. Normalized mean velocity profiles: (a) Weibull distribution fit and (b) logarithmic law. fig:weib

Table 1. Constants A_1 and A_2 in Eq. (1).

Author	A_1	A_2
Özdemir and Whitelaw (1992)	1.292	-6.2
Guerra et al. (2005)	1.124	-10.524
Present	0.962	-8.987

tab:A1A2

When the first term on the right-hand side of Eq. (6) is subtracted from the velocity profiles, the resulting curves collapse in a certain region (Fig. 2b), where they show the behaviour of an equilibrium layer.

As mentioned before, few works published in literature for impinging jets present data for the skin-friction coefficient. Notable contributions are the papers of Özdemir and Whitelaw (1992), Tu and Wood (1996), Phares et al. (2000) and Guo and Wood (2002). Özdemir and Whitelaw (1992) assessed the wall shear stress from observed streaks of pigmented oil which was sprayed uniformly over the experimental surface and exposed to the jet flow. Tu and Wood (1996) and Guo and Wood (2002) used Preston tubes and Stanton probes. For gas jets, Phares et al. (2000) observed the removal of monosized spheres.

Here, τ_w is evaluated from the slope of the linear velocity distribution in the viscous region. Velocity profiles at eight measuring positions are shown in Fig. 3a in inner coordinates. To every profile, at least five measurement points have been located in the first 250 μm of the wall. The resulting friction velocity distribution is shown in Fig. 3b together with results given by the Preston tube readings.

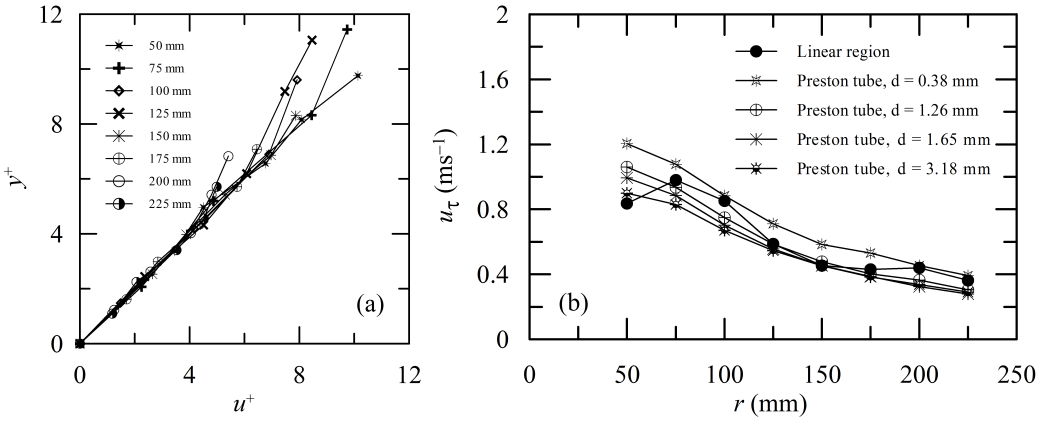

Figure 3. Velocity profiles in inner flow coordinates (a) and skin-friction velocity over the smooth impingement surface(b). fig:ulin

As far as the prediction of the wall shear stress is concerned, the work of Phares et al. (2000) follows the recommendation of some previous authors and suggests the flow domain for an impinging jet to be divided into four regions: the free-jet region, the inviscid impingement region, the impinging boundary layer and the wall-jet region. For the wall jet region, they use the empirical expression of Poreh et al. (1967) for the mean shear stress in a radial wall jet, Eq. (5).

Results yielded by Eq. (5) are shown in Fig. 4. In the jet deflection region, the strong streamline curvatures accelerate the boundary layer until the radial spreading starts to decelerate the flow giving rise to the wall-jet structure that was observed to begin development at about r = 75 mm. Figure 4 shows that for $4.0 < r/b < 10$ the empirical predictions of Eq. (5) show a good agreement with the experimental results. For $r/b < 4.0$, Eq. (5) predicts values that are within the order of magnitude of the experimental data but that disagree by as much as 50%.

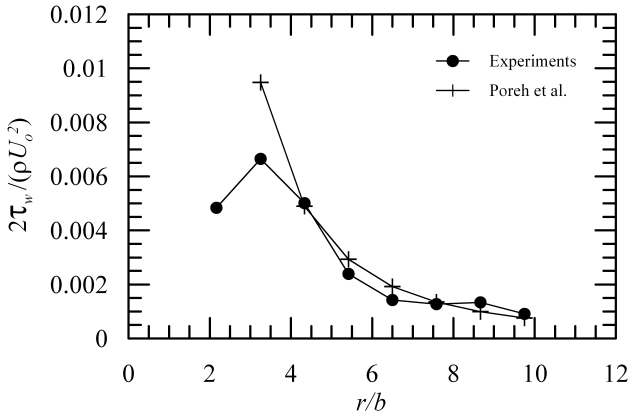

Figure 4. Wall shear stress distribution: present experimental data and predictions through the empirical expression of Poreh et al. (1967).

fig:wall

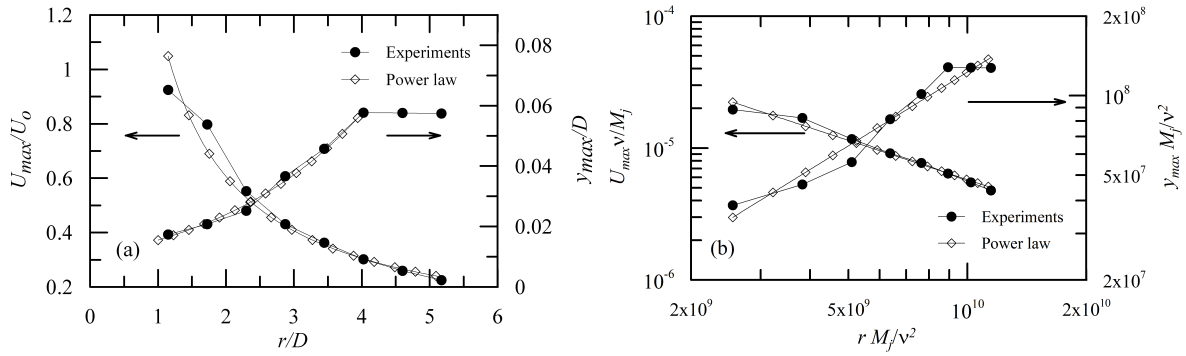

Figure 5. Functional behaviour of U_{max} and its position, y_{max}, as a function of the radial distance written in: (a) bulk variables and in (b) the variables proposed by Narasimha et al.(1973).

fig:umax

The description of the behaviour of U_{max} and its position, y_{max}, as a function of the radial distance is presented in Fig. 5a. Values quoted for parameters B_1, B_2, n_1 and n_2 in Eq. (3) vary greatly according to flow conditions. The data in Fig. 5a give B_1 = 1.203, n_1 = -0.989, B_2 = 0.010 and n_2 = 0.437 ($1 < r/D < 4$). Özdemir and Whitelaw (1992) found for their unconfined flow conditions, B_1 = 0.870, n_1 = -1.459, B_2 = 0.110 and n_2 = 1.156. In fact, in Özdemir and Whitelaw (1992), Eq. (3) was used to correlate $y_{0.5}$, the distance from the wall to the point $u = U_{max}/2$.

The choice of U_{max} and D as the basic flow scales has been challenged by Narasimha et al. (1973) with the argument of selective memory. These authors reason that sufficiently downstream in turbulent flows "the details of the initial conditions are not relevant, but rather only a few gross parameters which are in some sense dynamically equivalent".

Strictly speaking, Eqs. (4) should only be used for very large values of r/D. Figure 5b, however, shows that even for very small values of the radial distance, the power law fits perfectly well to the experimental data. The suggested values

of the flow parameters are: C_1 = 44974.65, m_1 = -0.989, C_2 = 0.064 and m_2 = 0.928. For the turbulent unconfined wall jet, Narasimha et al. (1973) report C_1 = 4.6, m_1 = -0.506, C_2 = 0.096 and m_2 = 0.91.

The exponents for Eqs. (3) and (4) were found to be exactly the same, -0.989, and this is a good indication that U_{max} presents a nearly inversely linear decay with r, in any of the considered propositions. This conclusion does not agree with Özdemir and Whitelaw (1992) and Narasimha et al. (1973), who found respectively, -1.459 (unconfined impinging jet) and -0.506 (unconfined wall jet). The increase of y_{max} with r in both propositions is proportional to the exponents 0.437 and 0.928 respectively. For n_2, Özdemir and Whitelaw (1992) estimated the value of 1.156, which does not agree with our present findings. However, the values of C_2 and m_2 published by Narasimha et al. agree almost exactly with our present measurements. This indicates that the growth of y_{max} is nearly linear with r in the gross parameter formulation of Narasimha et al. (1973).

The values of the outer peak in the local profiles of the rms value of u' (denoted $(u'_{rms})_{max}$) as compared to the peak values of the mean radial velocity and the friction-velocity are shown in Fig. 6 in physical coordinates. Of course, all these quantities decrease as r increases. However, and again, as expected, their decay rates are different. The peak in u'_{rms} is more persistent.

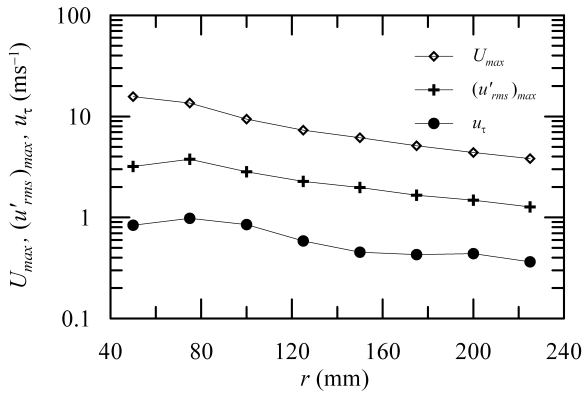

Figure 6. Behaviour of $(u'_{rms})_{max}$ in relation to U_{max} and u_τ in physical coordinates. fig:uuma

The Reynolds stresses in turbulent boundary layers have always been correlated in terms of wall variables – that is to say in terms of u_τ – so that similarity can be assessed. Typically, the development of u'_{rms}/u_τ for zero-pressure gradient flows in various Reynolds number regime shows a weak dependency on Reynolds number based on the momentum defect thickness (Fernholz and Finley, 1996).

Figure 7a shows the development of $(u'_{rms})_{max}$ normalized with u_τ, U_{max} and U_o. The dashed curves correspond to a straight line fit through the data of $(u'_{rms})_{max}/U_{max}$ and to a power law fit through the data of $(u'_{rms})_{max}/U_o$. The positions at which the u'-profiles reach the outer maximum, y'_{max}, are shown in Fig. 7b as expressed by Eq. (3).

The corresponding expressions are:

$$\frac{(u'_{rms})_{max}}{U_{max}} = 0.0142\left(\frac{r}{D}\right) + 0.2696, \tag{7}$$ eq:uumax

$$\frac{(u'_{rms})_{max}}{U_o} = 0.376\left(\frac{r}{D}\right)^{-0.969}. \tag{8}$$ eq:uumax

The linear behaviour of $(u'_{rms})_{max}/U_{max}$, with a slope that is about 1/20 of the intercept, means that over short distances changes in $(u'_{rms})_{max}/U_{max}$ will be small; to every unit of r/D, changes in $(u'_{rms})_{max}/U_{max}$ will be about 5%.

Of course, an analysis based on the gross parameters proposed by Narasimha et al. (1973) can also be attempted to

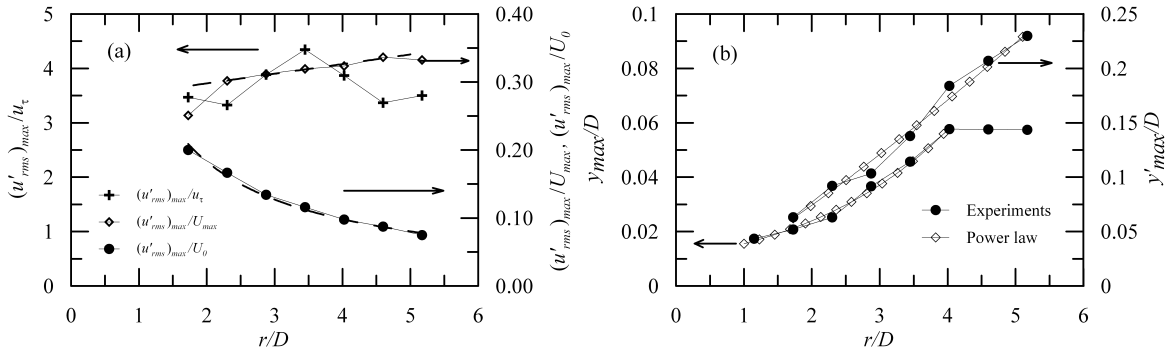

Figure 7. The distributions of: (a) $(u'_{rms})_{max}$ normalized with u_τ, U_{max} and U_o; (b) the radial distribution of y'_{max}. fig:uuma

correlate $(u'_{rms})_{max}$ and y'_{max}. In this case, we can write

$$\frac{(u'_{rms})_{max}\nu}{M_j} = D_1 \left(\frac{rM_j}{\nu^2}\right)^{m'_1}, \tag{9}$$ eq:u_rms

$$\frac{y'_{max}M_j}{\nu^2} = D_2 \left(\frac{rM_j}{\nu^2}\right)^{m'_2}. \tag{10}$$ eq:ymax_

The corresponding results are shown in Fig. 8. The power law fits furnish D_1 = 9095.45, m'_1 = 0.969, D_2 = 0.000412, m'_2 = 1.203. The worth comment here is that the exponents in Eqs. (8) and (9) are identical up to the third decimal.

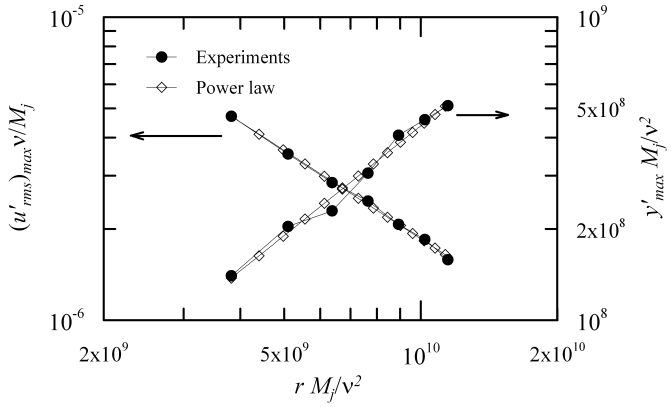

Figure 8. Functional behaviour of $(u'_{rms})_{max}$ and its position, y'_{max}, in the variables proposed by Narasimha et al. (1973). fig:u_rm

5. FINAL REMARKS

The results provided by the experimental characterization of the impinging jet were used to perform a scaling analysis of the problem based on propositions that resort to classical variables such as the nozzle diameter, nozzle-to-plate space and bulk velocity of the jet. An alternative analysis was made considering some gross parameters of the jet such as its momentum flux. A discussion on the behaviour of U_{max} and u'_{rms} and their locations y_{max} and y'_{max} in terms of the non-dimensional power law expressions has also been made. It has been shown that U_{max} presents an inversely linear decay with the radial distance whereas y_{max} grows almost linearly with r. This indicates that the jet momentum flux M_j may actually be a very appropriate flow scaling for the parametric representation of impinging jets.

6. ACKNOWLEDGEMENTS

In the course of the research, JBRL benefited from a CNPq Research Fellowship (Grant No 301172/2010-2) and from further financial support through Grant 477354/2011-4. APSF is grateful to the Brazilian National Research Council (CNPq) for the award of a Research Fellowship (Grant No 303982/2009-8). The work was financially supported by CNPq through Grants No 477293/2011-5 and by the Rio de Janeiro Research Foundation (FAPERJ) through Grant E-26/102.937/2011.

7. REFERENCES

Fernholz, H. H. and Finley P. J., 1996. The incompressible zero-pressure-gradient turbulent boundary layer: an assessment of the data, Prog. Aero. Sci., vol. 32, 245-311.

Guerra, D. R. S., Su, J. and Silva Freire, A. P., 2005. The near wall behaviour of an impinging jet. Int. J. Heat and Mass Transfer, vol. 48, 2829-2840.

Guo, D. Y. and Wood, D. H., 2002. Measurements in the vicinity of a stagnation point, Exp. Thermal and Fluid Sciences, vol. 25, 605-614.

Loureiro, J. B. R., Sousa, F. B. C. C., Zotin, J. L. Z. and Silva Freire, A. P., 2010. The distribution of wall shear stress downstream of a change in roughness, International Journal of Heat and Fluid Flow, vol. 31, pp. 785–793.

Narasimha, R., Narayan, K. Y. and Pathasarathy, S. P., 1973. Parametric analysis of turbulent wall jets in still air. Aeronautical Journal, vol. 77, pp. 335–339.

Özdemir, I. B. and Whitelaw, J. H., 1992. Impingement of an axisymmetric jet on unheated and heated flat plates. Journal of Fluid Mechanics, vol. 2, pp. 503–532.

Phares, D. J., Smedley, G. T., Flagan, R., 2000. The wall shear stress produced by the normal impingement of a jet on a flat surface, J. Fluid Mech. vol. 418, pp. 351-375.

Poreh, M., Tsuei, Y. G. and Cermak, J. E., 1967. Investigation of a turbulent radial wall jet. Trans. ASME: Journal of Applied Mechanics, vol. 34, pp. 457–463.

Tu, C. V. and Wood, D. H., 1996. Wall pressure and shear stress measurements beneath an impinging jet, Exp. Thermal Fluid Science, vol. 13, pp. 364-373.